Particle size distribution of pretreated oilseeds affects cumulative supercritical CO_2 extraction plots

José M. del Valle[a,*], Constanza V. Carrasco[a], Felipe R. Toledo[a], & Gonzalo A. Núñez[b]

[a] Depto. Ing. Química y Bioprocesos, Pontificia Universidad Católica de Chile, Santiago
[b] Depto. Ing. Química y Ambiental, Campus San Joaquín, Univ. Técnica Federico Santa María, Santiago, Chile
[*] delvalle@ing.puc.cl

ABSTRACT

Typically, SuperCritical (SC) carbon dioxide (CO_2) extraction of pretreated oilseeds in a packed bed assumes a single particle size and shape, but this may not apply at the industrial scale for which operational conditions are not as closely adjusted as in the laboratory or pilot plant. The objective of this work was to study the effect of the particle size distribution of the substrate on the SC-CO_2 extraction of oil from pelletized seeds experimentally and using mathematical simulation. Cranberry seeds were treated to produce cylindrical pellets of same height and diameter, corresponding to their equivalent diameter (d_{pe}). Samples of small (d_{pe} = 2 mm), large (d_{pe} = 4 mm), and 1:1 (w/w) mixture (**M**) of small (**S**) and large (**L**) pellets were extracted in triplicate for 3 h in a 200-cm^3 extraction vessel using 25 g/min of SC-CO_2 at 40 ºC and 30 MPa. Cumulative extraction curves for the S and L samples were modeled simultaneously using the Linear Driving Force (LDF) model modified to consider the oil partition isotherm experimentally determined for prepressed oilseeds, and using oil solubility in SC-CO_2 (C_{sat}) and the effective diffusivity of the oil in the substrate (D_e) at process conditions (40 ºC and 30 MPa) as the two best-fitting parameters. The mathematical model was adapted for a substrate with a particle size distribution, in which individual extraction rates are determined by the LDF model for each size fraction as a function of extraction time and axial position in the packed bed considering the single concentration of the oil in the CO_2 at that time and position. Then, it was used to simulate the experimental cumulative extraction curve of the **M** sample with the values of C_{sat} and D_e estimated for samples **S** and **L**. Simulated and experimental results agreed, thus validating our model for polydisperse substrates. The mathematical model was subsequently extended to simulate the SC-CO_2 extraction of substrates with different particle size distributions (characterized by differences in dispersion and skewness of normal distributions). We observed that the extraction plots of substrates with the same measurement of central tendency (Sauter mean diameter) changed depending on the particle size distribution.

INTRODUCTION

Mathematical simulation is a useful tool to estimate total production and production costs of a SuperCritical (SC) Fluid Extraction (SCFE) plant depending on substrate and process conditions [1−3]. These simulations demand mathematical models capable of describing the mass transfer within solid substrates, as well as dealing with the nuances of the pretreatments of biological (*e.g.*, vegetable) matrices. This implies they should be capable of dealing with 'non-ideal' conditions in the extraction vessel that do not fit common assumptions of mathematical model. When modelling SCFEs it is commonly assumed that the packed bed consists of monosized particles. Although in laboratory experiments substrate particles may be size-classified after milling so as to be within a narrow interval, it is unrealistic to assume that noncomplying particles are discarded at the industrial level. Possibly the industrial substrate is subjected to a standardized size-reduction procedure that achieves a given grade that is characterized by a wider interval of particle sizes, as done by Sovová [4] for grape seeds. In these cases, the particle size (d_p) can be reduced to an average value such as the Sauter mean diameter (S_{md}).

Fiori *et al.* [5] showed that adopting S_{md} instead of the real particle diameters is adequate only in cases

where the size distribution exhibits a small variance. This was not the case when the difference in size between the smallest (0.40-mm) and largest (1.62-mm) particle was large and the difference between the simulated extraction curve a 1:1 (w/w) mixture of the two and a monosized sample with same S_{md} were of up to 10% [5]. This will occur whenever there is a portion of dust-like particles whose oil is easily depleted in the initial stages of the extraction process, which is always possible, even if sample pretreatment considers size classification by sieving, because of the tendency of dust-like particles to adhere to larger particles [6,7]. Sovova [8] concluded that the experimental results of Sovova *et al.* [4] for the extraction of milled grape seeds with a wide size distribution should be analyzed using a polydisperse model such as those proposed by Fiori *et al.* [5] or Egorov *et al.* [6] to avoid unrealistic values of the inner mass transfer coefficient.

The objective of this work was to study the effect of the particle size distribution of the substrate on the SC-CO_2 extraction of oil from pelletized seeds using experimental and mathematical simulation tools.

MATERIALS AND METHODS

Substrate

Cranberry (*Vaccinium oxycoccus*) fruit seeds provided by Granasur (Santiago, Chile) were used as substrate. Seeds were pretreated in a flat D-type pellet mill having exchangeable die openings (2- and 4-mm diameter). The extruded material was manually cut into cylindrical pellets having a unitary height (h)-to-diameter (d) ratio. We formed three kinds of packed beds with small ($h = d$ = 2 mm), large ($h = d$ = 4 mm), and 1:1 (w/w) mixture (**M**) of small (**S**) and large (**L**) pellets. Samples were kept in sealed plastic bag in a refrigerator up to the time of analysis.

Supercritical CO_2 extraction experiments

For each extraction, 120 g of pellets (samples **S**, **L**, or **M**) were loaded into a 200 cm^3 extraction vessel (inner diameter, D = 5 cm). The vessel was placed in a temperature-controlled air convection oven set at 40 ºC. The one-pass system was fed with a piston pump and the system pressure kept at the set value of 30 MPa using an automated back-pressure regulator. Extractions were carried out using 99.8% pure CO_2. Following 90 min of static extraction to equilibrate system conditions at the desired set values, the dynamic extraction period was initiated setting the pump in the flow-control mode to pass 20 g/min of CO_2 at 40 ºC and 30 MPa (superficial velocity, U = 0.19 mm/s) through the extraction vessel for *ca.* 210 min. All experiments were performed in triplicate.

During dynamic extraction, oil aliquots were collected in pre-weighed cleaned and dried glass vials (10 to 12 depending on the experiment). The vials were kept up to constant weight in a desiccator with dried silica gel to remove co-extracted water from the samples. The amount of extracted oil in each time interval was estimated gravimetrically by difference with the clean and empty glass vials.

Both the moisture and oil content of the original and the extracted pellets were measured and the recovery of oil was estimated by comparing the amount collected in the glass vials, with the difference in oil content between the original and treated substrate evaluated in a moisture-free and oil-free basis (to circumvent weight changes associated with SC-CO_2 extraction). For computations, the moisture content was measured gravimetrically by removing water from representative samples by drying in an oven set at 105 ºC for 72 h. The oil content, on the other hand, was also measured gravimetrically by extracting representative samples to exhaustion in a Soxhlet apparatus using technical grade hexane. Hexane was removed from the extract by rotaevaporation and the round bottom flask was placed in the desiccator to remove residual traces. The overall oil recovery value of each experiment was considered when constructing the cumulative extraction plot of oil yield *versus* specific CO_2 consumption.

Mathematical modeling and simulation of supercritical CO_2 extractions

− *Static extraction stage*. For this stage equilibrium was assumed between the pelletized substrate and the SC-CO_2 in the extraction vessel, with the end result of partition of the oil between the two phases according to the equilibrium isotherm experimentally determined for prepressed oilseeds [9]:

$$C_{fo} = C_{sat}\left[\alpha\, C_{so} + \left(1-\alpha\, C_{so}\right)\frac{\left(C_{so}\right)^{n}}{A+\left(C_{so}\right)^{n}}\right], \quad (1)$$

where C_{fo} (g kg^{-1} oil/CO_2) and C_{so} (g kg^{-1} oil/substrate) are the equilibrium concentrations of oil in SC-CO_2 and the substrate, respectively; C_{sat} (g kg^{-1} oil/CO_2) is the solubility of oil in SC-CO_2 at process conditions; and α (0.4912), A (1.9×10^{-5}), and n (3.34) are model parameters that were extrapolated to process conditions using the expressions proposed by Urrego *et al.* [9]. In addition, the amount of oil originally in the substrate (initial concentration C_o, g kg^{-1} oil/substrate) is kept within the extraction vessel, which is stated by the mass conservation equation:

$$C_o - C_{so} = \frac{\rho}{\rho_s}\left(\frac{\varepsilon}{1-\varepsilon}\right)C_{fo}, \quad (2)$$

where ρ (kg/m^3) is the density of the SC-CO_2 at process conditions; ρ_s (kg/m^3) is the particle density, that can be estimated as the ratio of the weight and apparent volume of the cylindrical pellets; and ε is the porosity of the bed, that can be estimated as a function of D/d_p for a packed bed of cylinders using the equation of Benyahia and O'Neill [10].

Simultaneous resolution of Eq. (1) and Eq. (2) determined the initial concentrations of oil in the two phases, C_{fo} and C_{so}, in the extraction vessel.

− *Dynamic extraction stage*. Cumulative extraction curves during the dynamic extraction stage were modeled using the Linear Driving Force (LDF) model [11], which was adapted for a substrate with polydisperse substrate having a known particle size distribution, as shown in Eq. (3) that describes the differential mass conservation in packed bed in the absence of axial dispersion phenomena, and Eq. (4) that describes the rate of transfer of oil from substrate fraction "i" to the flowing CO_2 stream.

$$\frac{\partial C_f}{\partial t} = -\left(\frac{U}{\varepsilon}\right)\frac{\partial C_f}{\partial z} + \left(\frac{1-\varepsilon}{\varepsilon}\right)\sum_{i=1}^{N} w_i k_{p,i} a_{p,i}\left(C_{f,i}^{*} - C_f\right), \text{ and} \quad (3)$$

$$\frac{\partial C_{s,i}}{\partial t} = -\frac{\rho}{\rho_s} k_{p,i} a_{p,i}\left(C_{f,i}^{*} - C_f\right) \quad \forall\ i \in 1...N, \quad (4)$$

where t (s) is the extraction time; z (m) is the axial coordinate; ω_i (−) is the mass fraction of substrate particles with average size "i"; N is the number of fractions in the particle size distribution; C_f (kg/m^3) is the concentration of oil in the SC-CO_2 phase; $C_{s,i}$ (kg/m^3) is the concentration oil in substrate particles with average size "i"; $C_{f,i}^{*}$(kg/m^3) is the concentration of oil in SC-CO_2 that is in equilibrium with a substrate containing $C_{s,i}$ of oil, Eq. (5a); $k_{p,i}$ (m/s) is the global mass transfer coefficient for particles with average size "i", Eq. (5b); $a_{p,i}$ (m^2/m^3) the specific surface of particles with average size "i", Eq. (5c):

$$C_{f,i}^{*} = C_{sat}\left[\alpha\, C_{s,i} + \left(1-\alpha\, C_{s,i}\right)\frac{\left(C_{s,i}\right)^{n}}{A+\left(C_{s,i}\right)^{n}}\right], \quad (5a)$$

$$k_{p,i} = \frac{10\, k_{f,i}}{10 + \frac{k_{f,i} d_{p,i}}{D_e}}, \text{ and} \quad (5b)$$

$$a_{p,i} = \frac{6}{d_{p,i}}. \quad (5c)$$

Eqs. (4) and (5) express that the oil from each size fraction in the extraction vessel is being extracted at a particle-size-dependent rate that depends on its individual residual oil content ($C_{s,i}$), film mass transfer coefficient ($k_{f,i}$), and surface-to-volume ratio ($a_{p,i}$). On the hand, it is implicitly assumed that the effective

diffusivity of the oil in the substrate (D_e) is constant.
To solve differential equation Eq. (3) and Eq. (4), we considered as the initial conditions that there were equilibrium conditions in the extraction vessel at the end of the static extraction period, Eq. (6a) and Eq. (6b), and as the boundary condition that there was no dissolved oil in the CO_2 entering the extraction vessel, Eq. (6c):

$$C_f\big|_{t=0,z} = C_{fo}, \tag{6a}$$

$$C_{s,i}\big|_{t=0,z} = C_{so} \quad \text{" i Î } 1...N, \text{ and} \tag{6b}$$

$$C_f\big|_{t,z=0} = 0. \tag{6c}$$

To simulate the cumulative extraction curve we solved Eq. (7) using Eq. (8) as the initial condition:

$$\left.\frac{dY}{dt}\right|_t = \frac{G}{M_s} C_f\big|_{t,z=L}, \text{ and} \tag{7}$$

$$Y\big|_{t=0} = 0, \tag{8}$$

where Y (g kg^{-1} oil/substrate) is the extraction yield; G (kg/s) is the volumetric flow rate of CO_2 at process conditions; and M_s (kg) is the substrate load of the extraction vessel.

− *Model parameters*. The physical properties of the SC-CO_2 and film mass transfer coefficients were estimated by applying a literature procedure under process conditions [12]. The density (ρ = 909.9 kg/m^3) and viscosity ($\mu = 9.38\times10^{-5}$ Pa s) of the SC-CO_2 was estimated using the REFPROP program [13] for pure CO_2 at 40 ºC and 30 MPa under the assumption that the dissolved oil (low solubility) does not affect them. The binary diffusion coefficient of the oil in SC-CO_2 ($D_{12} = 3.02\times10^{-9}$ m^2/s) was estimated using the correlation of Funazukuri *et al*. [14] using triolein as a representive component in the vegetable oil [12]. Finally, values of $k_{f,i}$ were estimated using the dimensionless correlation of King and Catchpole [15] for the Sherwood number [*Sh*, Eq. (9a)] as a function of the as a function of the Schmidt number (*Sc* = 34.2) and the particle-size-dependent Reynolds number [*Re*, Eq. (9b)]:

$$Sh_i = \frac{k_{f,i} d_{p,i}}{D_{12}}, \text{ and} \tag{9a}$$

$$Re_i = \frac{\rho\, U\, d_{p,i}}{\mu}. \tag{9b}$$

The mathematical model was adapted for a monosized substrate and fitted simultaneously for samples **S** and **L** using single values of C_{sat} and D_e as best fitting parameters. Then, it was adapted for a bisized substrate and used to simulate the cumulative extraction curve of sample **M** ($\omega_1 = \omega_2 = 0.5$, d_{p1} = 2 mm, d_{p2} = 4 mm) with the previously determined values of C_{sat} and D_e. Thus, it was use as a fully predictive model for validation purposes.

− *Application*. The modified LDF model was extended to simulate the SC-CO_2 extraction of substrates with different particle size distributions to characterize the effect of the dispersion and skewness on the cumulative extraction curves. Different particle size distributions were generated using the normal-skew distribution [16]. The density function of this probability distribution is given by Eq. (10):

$$f(x) = \frac{2}{\sqrt{2\pi\, w^2}} \exp\left[-\left(\frac{x-\xi}{\sqrt{2}\, w}\right)^2\right] \int_{-\infty}^{\alpha(x-\xi)/w} \frac{1}{\sqrt{2\pi}} \exp\left[-\frac{t^2}{2}\right] dt, \tag{10}$$

where ξ corresponds to a location parameter that, in the case of normal distribution, equals the average of the data; w is the scale parameter corresponding to the standard deviation in normal distribution; and α is the parameter of asymmetry (shape) that equals zero in the normal distribution. For application, we

discretized the distributions in N = 18 size classes whose frequency was characterized by the value given by Eq. (10) in the middle point that covered a total interval for which predicted frequencies were above a limiting threshold. To study the effect of the shape of the distribution we selected parameter values in Eq. (10) for a normal distribution (**N**) and two normal-skew distributions with negative (**−S**) and positive (**+S**) skewness that resulted is discretized distributions with the same value of S_{md} [Eq. (11a)] and same range [R, Eq. (11b)] or interval between the smallest and largest particle size:

$$S_{md} = \left(\sum_{i=1}^{N} \frac{w_i}{d_{p,i}} \right)^{-1}, \text{ and} \tag{11a}$$

$$R = d_{p,max} - d_{p,min}. \tag{11b}$$

To study the effect of the range we selected parameters for a normal distribution, that we called sample **W**, which had the same value of S_{md} as sample **N** but a much larger range. The selected value of S_{md} was 2.67 mm that coincides with experimental sample **M**.

RESULTS

Fig. 1 presents experimental, best-fitted, and simulated cumulative extraction curves for packed beds of samples **L**, **M**, and **S**. A single set of values of C_{sat} = 19 g kg^{-1} oil/CO$_2$ and D_e = 6.06×10^{-10} m^2/s represented experimental data for samples **S** and **L** quite well. The value of C_{sat} is higher than values extrapolated by Urrego *et al.* [9] for rapeseed oil at 40 ºC and 30 MPa (9.5 g kg^{-1} oil/CO$_2$) as well as predicted by del Valle *et al.* [17] for typical vegetable oil at the same conditions (8.1 ± 2.4 g kg^{-1} oil/CO$_2$). Although most vegetable oils are of the C-54 type, or triacylglycerol of fatty acids of 18 carbon atoms [17], there is some oil-to-oil variability that may explain the ±30% estimated error band reported by del Valle *et al.* [17]. Furthermore, hydrolytic deterioration of the oil liberation of fatty acids from the triglycerides may increase the solubility in SC-CO$_2$, as observed by Sovova *et al.* [18] for the grape seed oil they used. We did not measure the acidity of the cranberry seed oil we extracted at the time we made our experiments to confirm this hypothesis.

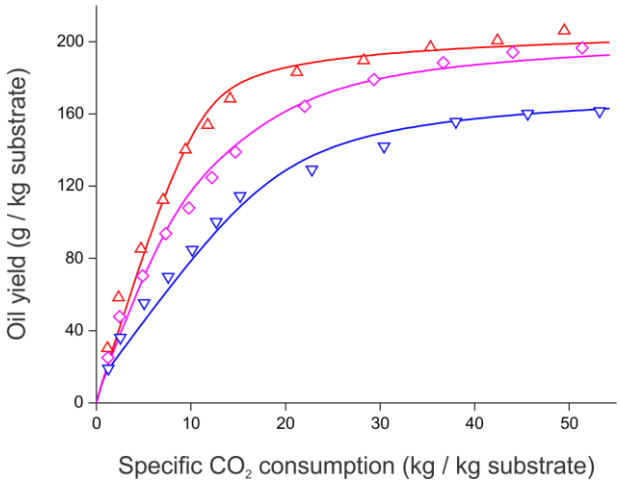

Figure 1. Cumulative extraction curves for the SC-CO$_2$ extraction of packed beds of pelletized cranberry seeds at 40 ºC and 30 MPa. Symbols indicate experimental data for samples (△) **S**, (▽) **L**, and (◇) **M**, whereas continuous lines of same color represent simulated curves using the modified LDF model. The simulated curve for sample **M** is predictive because no fitting parameter was used.

A single value of D_e for the extraction of pelletized cranberry seeds gives validity to the assumption that the pretreatment in the D-type pellet mill causes similar disruption of the cellular tissue of the cranberry seeds at the microstructural level, regardless of the diameter of the die openings. The shearing of the seed tissue in the pellet mill frees the oil from cells facilitating extraction. Considering the binary diffusion coefficient of the oil in SC-CO$_2$, a microstructural factor (F_m, or the ratio D_{12}/D_e) of 4.97 can be estimated

for the pelletized cranberry seeds, which is of the same order of magnitude estimated by del Valle *et al.* [20] for several oilseed samples subjected to high-shear prepressing and flaking pretreatments ($3.4 \leq F_m \leq 33$).

It is remarkable that model parameters estimated using cumulative extraction curves for samples **S** and **L** can predictively simulate the cumulative extraction curve of sample **M** with great precision (Fig. 1). To the best of our knowledge this is the first time that a polydisperse model is applied to the SC-CO_2 of a packed bed of a solid substrate without resorting to best-fitting selected model parameters.

Table 1 presents the parameters we used to generate the four particle size distributions in Fig. 2A having the same Sauter diameter as sample **M** (S_{md} = 2.67 mm) using Eq. (10).

Table 1. Parameters used in Eq. (10) for each generated particle size distribution.

Parameter	Particle size distribution			
	N	**-S**	**+S**	**W**
x (mm)	1.670 – 3.730	2.165 – 4.230	1.200 – 3.260	0.215 – 5.875
R (mm)	2.061	2.065	2.061	5.066
ξ (mm)	2.7042	2.2233	3.2059	3.0499
w (mm)	0.308	0.600	0.600	0.950
α (−)	0.0000	-0.9907	0.9907	0.0000

For the discretization of samples **N** and **W**, all size classes had the same width of was the same (R/18), and size classes 8 and 9 shared a side corresponding to the highest frequency size (the mean of the normal distribution). The width of the size classes for samples **−S** and **+S** varied depending on the local steepness of distribution, as illustrated for sample **−S** in Figs. 2B and 2C. There were two central size classes of width R/37.5 that shared a side corresponding to the highest frequency size, five size classes of width R/167 at the steep side of the two central classes, and eleven size classes of width R/12.0 at the gradual side of the two central classes. Using this discretization we were able to capture the essential feature of the normal-skew distributions we selected. We ensured that the sum of all size fractions was one by defining the weight fractions a indicated in Eq. (12), where function $f(x)$ is defined by Eq. (11):

$$w_i = \left(\frac{d_{p,i} - d_{p,i-1}}{A} \right) f\left(\frac{d_{p,i-1} + d_{p,i}}{2} \right), \tag{12}$$

where $A = \sum_{i=1}^{18} \left(d_{p,i} - d_{p,i-1} \right) f\left(\frac{d_{p,i-1} - d_{p,i}}{2} \right)$, $d_{p,0} = d_{p,min}$, and $d_{p,18} = d_{p,max}$.

Fig. 3 shows the cumulative extraction curves for simulated SC-CO_2 extraction of cranberry seeds using the generated particle size distributions. The same as in our experiments, regardless of the size distribution all cumulative extraction curves coincide initially because of the influence of the static extraction stage where a particle-size-independent equilibrium is reached between the substrate and SC-CO_2. The narrow distributions (**−S**, **M**, and **+S,** R = 2.06-2.07 mm) remain close up to about 15 kg kg^{-1} CO_2/substrate and then extraction rates start to deviate slightly in favor of that distribution having a proportion of smaller particles. As compared to the normal distribution (**N**), after using 55 kg kg^{-1} CO_2/substrate the yield of sample **−S** is about 3% higher, whereas that of sample **+S** is 2.5% lower. When the distribution widens (R = 5.07 mm for sample **W**) so does the difference in extraction yield as compared to a narrower distribution (R = 2.06 mm for sample **N**) particularly at intermediate specific solvent consumptions between 7.5 and 35 kg kg^{-1} CO_2/substrate, and this coincides with the observation of Fiori *et al.* [5]. According to these authors, after a short period of time the yield of the sample having larger particles becomes smaller because of the delayed extraction of tied solute from the largest

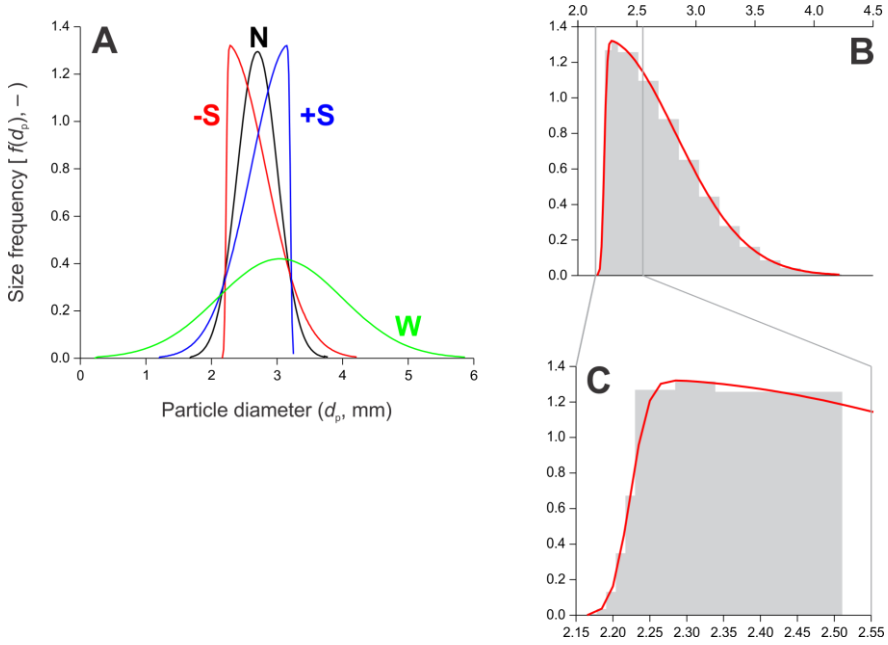

Figure 2. (A) Particle size distributions generated using parameter values in Table 1. **(B)** Discretized particle size distribution for the negatively-skewed distribution (sample **–S**). **(C)** Zoom of (B) showing classes within the size range 2.15−2.55 mm.

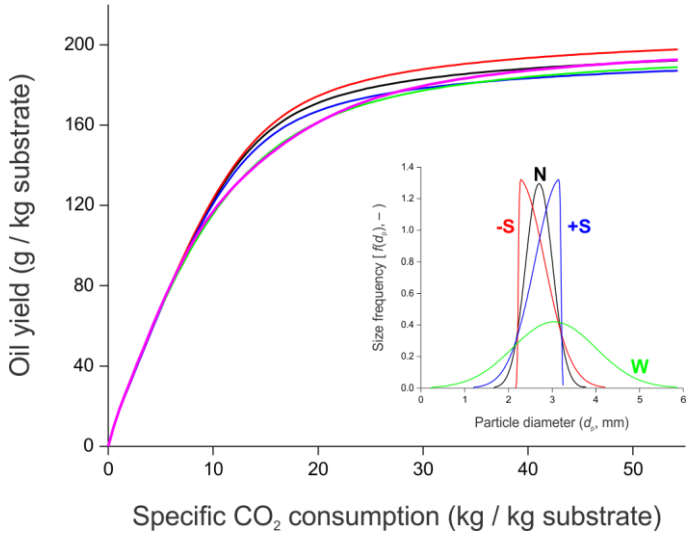

Figure 3. Simulated cumulative extraction curves for the extraction of pelletized oilseeds using SC-CO_2 at 40 ºC and 30 MPa from the discretized particle size distributions in Table 1 (magenta line is the simulated curve for experimental sample **M**).

particles. The cumulative extraction curve of sample **M** is similar to that of sample **W** up the time when 20 kg kg^{-1} CO_2/substrate are used and from then on it steadily approaches that of sample.

CONCLUSIONS

Our main conclusion are that it is possible describing the extraction of pelletized oilseeds using the LDF model modified to use the equilibrium partition of oil between prepressed canola seeds and SC-CO_2, as well modifying the model to account for the particle size distribution of the substrate, and that the cumulative extraction curve of a substrate having a wide distribution of particle size is not well represented by the extraction of a monosized sample having the same Sauter mean diameter.

ACKNOWLEDGEMENTS

This work was funded by Chilean scientific agency FONDECYT (Project #1150623).

REFERENCES

[1] DEL VALLE J.M., NUÑEZ G.A., ARAVENA R.I., Supercritical CO_2 oilseed extraction in multi-vessel plants. 1. Minimization of operational cost, Journal of Supercritical Fluids, Vol. 92, 2014, p. 197–207.

[2] NUÑEZ G.A., DEL VALLE J.M., Supercritical CO_2 oilseed extraction in multi-vessel plants. 2. Effect of number and geometry of extractors on production cost, Journal of Supercritical Fluids, Vol. 92, 2014, p. 324–334, 2014.

[3] NUÑEZ G.A., DEL VALLE J.M., NAVIA D., Supercritical CO_2 oilseed extraction in multi-vessel plants. 3. Effect of extraction pressure and plant size on production cost, Journal of Supercritical Fluids, Vol. 122, 2017, p. 109–118.

[4] SOVOVA H., Rate of the vegetable oil extraction with supercritical CO_2-I. Modelling of extraction curves, Chemical Engineering Science, Vol. 49, 1994, p. 409–414.

[5] FIORI L., BASSO D., COSTA P., Seed oil supercritical extraction: Particle size distribution of the milled seeds and modeling, Journal of Supercritical Fluids, Vol. 47, 2008, p. 174–181.

[6] EGOROV A.G., MAZO A.B., MAKSUDOV R.N., Extraction from a polydisperse granular layer of milled oilseeds with supercritical carbon dioxide, Theoretical Foundations of Chemical Engineering, Vol. 44, 2010, p. 642–650.

[7] EGOROV A.G., SALAMATIN A.A., Bidisperse shrinking core model for supercritical fluid extraction, Chemical Engineering & Technology, Vol. 38, 2015, pp. 1203–1211.

[8] SOVOVÁ H., Steps of supercritical fluid extraction of natural products and their characteristic times, Journal of Supercritical Fluids, Vol. 66, 2012, p. 73–79.

[9] URREGO F.A., NÚÑEZ G.A., DONAIRE Y.D., DEL VALLE J.M., Equilibrium partition of rapeseed oil between supercritical CO_2 and prepressed rapeseed, Journal of Supercritical Fluids, Vol. 102, 2015, p. 80–91.

[10] BENYAHIA F., O'NEILL K.E., Enhanced voidage correlations for packed beds of various particle shapes and sizes, Particulate Science and Technology, Vol. 23, 2005, p. 169-177.

[11] DEL VALLE J.M., DE LA FUENTE J.C., Supercritical CO_2 extraction of oilseeds: Review of kinetic and equilibrium models, Critical Reviews in Food Science and Nutrition, Vol. 46, 2006, p. 131-160.

[12] DEL VALLE J.M., Extraction of natural compounds using supercritical CO_2: Going from the laboratory to the industrial application, Journal of Supercritical Fluids, Vol. 96, 2015, p. 180–199.

[13] LEMMON E.W., HUBER M.L., MCLINDEN M. O., NIST Standard Reference Database 23: Reference Fluid Thermodynamic and Transport Properties (REFPROP), Version 9.1, National Institute of Standards and Technology, Standard Reference Data Program, Gaithersburg, 2013.

[14] FUNAZUKURI T., TORIUMI M., YUI K., KONG C.Y., KAGEI S., Correlation for binary diffusion coefficients of lipids in supercritical carbon dioxide, in: 9th International Symposium on Supercritical Fluids (ISSF 2009), 2009, p. May 18-20.

[15] KING M.B., CATCHPOLE O., Physico-chemical data required for the design of near-critical fluid extraction processes, in: KING M.B, BOTT T.R. (eds.), Extraction of Natural Products Using Near-Critical Solvents, Blackie Academic & Professional, London, UK, 1993, p. 184–231

[16] AZZALINI A., The Skew-Normal and Related Families, Cambridge University Press, 2013.

[17] DEL VALLE J.M., DE LA FUENTE J.C., UQUICHE E., A refined equation for predicting the solubility of vegetable oils in high-pressure CO_2, Journal of Supercritical Fluids, Vol. 67, 2012, p. 60–70.

[18] SOVOVA H., ZAREVUCKA M., VACEK M., STRANSKY K., Solubility of two vegetable oils in supercritical CO_2, Journal of Supercritical Fluids, Vol. 20, 2001, p. 15-28.

[20] DEL VALLE J.M., GERMAIN J.C., UQUICHE E., ZETZL C., BRUNNER G., Microstructural effects on internal mass transfer of lipids in prepressed and flaked vegetable substrates, Journal of Supercritical Fluids, Vol. 37, 2006, p. 178-190.